Transactions, SMiRT-23
Manchester, United Kingdom - August 10-14, 2015
Division II, Paper ID 189
(Fracture Mechanics and Structural Integrity)

VALIDATION OF A FRACTURE MECHANICS APPROACH FOR THE FAST FRACTURE EVALUATION OF DISSIMILAR METAL WELDS

Arnaud Blouin[1], Stéphane Chapuliot[2], and Stéphane Marie[3]

[1] Research & Development Engineer, AREVA NP, France (arnaud.blouin@areva.com)
[2] Expert in Fracture Mechanics, AREVA NP, France (stephane.chapuliot@areva.com)
[3] Expert in Fracture Mechanics, AREVA NP, France (stephane.marie@areva.com)

ABSTRACT

This article presents the current status on the effort performed within AREVA in support of the Fracture Mechanics Assessment approach under development for the justification of Dissimilar Metal Welds. It follows a first step presented in a previous paper and devoted to the validation of the J parameter calculation through a Finite Element (F.E.) modelling for a crack at the interface between two different materials.
This paper focuses on the residual stress field consideration within the F.E. modelling: how to define the residual stress field to consider in the model, how to introduce it in the model and how relevant are the calculated values.
In a first part, the main obtained results from the previous paper are reminded. Afterwards, the definition of the residual stress field is discussed. It basically relies on residual stress measurements and numerical welding simulation but it has to be specifically adapted for the F.E. modelling purpose. Following this definition step, a protocol for the introduction of those stresses within the model and a parametric study on the residual stress distribution are proposed. Here, the model is 2D and thus allows a fast and accurate sensitive study. As a conclusion, several perspectives are discussed from that parametric study.

INTRODUCTION

Fast fracture analysis of dissimilar metal welds (DMW), in particular the characterization of the usual parameters such as the *J* parameter, constitutes a well-known problematic in Fracture Mechanics and a major challenge for nuclear industry. In that paper, we are considering a narrow gap dissimilar metal weld (DMW), typical of the welds between the ferritic steel main components of the primary circuit and the austenitic steel piping system of the EPR™. The weld is made of nickel based alloy (Inconel 52). A conventional crack is postulated at the interface between the nickel base alloy weld and the ferritic steel since this area was shown to have the lowest ductile toughness [1 to 3] and could present defects due to the welding process (Figure 1).
In order to characterize the toughness of the dissimilar metal weld in both brittle and ductile regimes, the *J* parameter is calculated for the considered crack through the G-Theta method. However, this configuration is very complex and it is necessary to check the numerical validity of such a calculation. Also, the demonstration was brought into a previous paper for a lot of different types of loadings, elastic and elastic-plastic materials behaviours and is very briefly presented. To complete that study, it has been decided to consider the presence of residual stresses which are due to the welding process that could exist in a DMW. First, it is proposed to determine a realistic, simple and conservative residual stress field for this kind of DMW. Then, in order to evaluate the impact of the distribution of a residual stress field, three different ones are defined with different levels of stress and both uniaxial and biaxial directions. A methodology to introduce correctly those residual stresses into FE models is proposed before proceeding to the analysis of the different obtained results. As a matter of fact, a parametric study has been performed using the FE code CASTEM® (used for R&D studies at AREVA) with elastic and elastic-plastic properties. Finally, the effect of residual stresses on *J* values is analysed for the different considered cases and the calculation of J is numerically validated.

DISSIMILAR METAL WELD AND MATERIALS PROPERTIES

In that paper, the narrow gap DMW (Figure 1) is representative of the weld between the EPR™ pressure vessel (A508 ferritic steel) and the coolant piping system (304L austenitic steel). The weld is made of nickel based alloy (Inconel 52) and there is a 304L cladding inside of the pressure vessel. For the F.E. calculations, dimensions of the corresponding 2D simplified structure are given in Table 1.

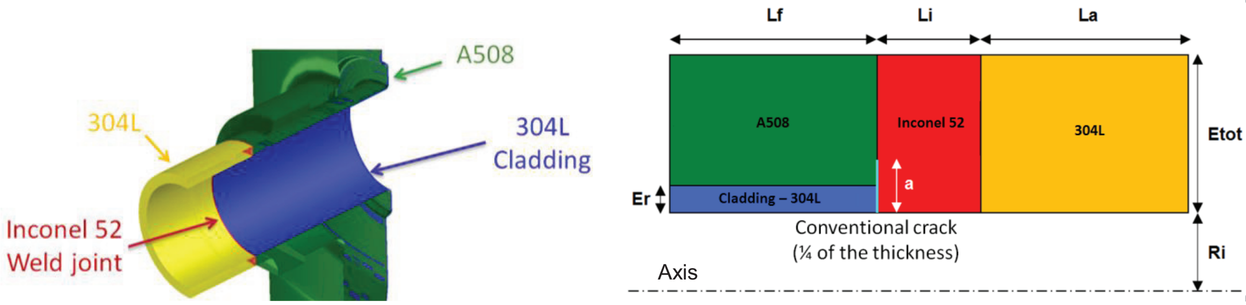

Figure 1. Structure and dissimilar metal weld

Table 1: General dimensions

Parameter	Dimension (mm)
L_f	700
L_i	10
L_a	690
E_r	10
E_{tot}	100
R_i	500
a	20

All materials are assumed to behave as isotropic elastic-plastic materials with material properties possibly varying with temperature. As an example, Figure 2 gives the tensile curves of the three different materials at 300 °C. The materials properties for all temperatures are not given in this paper for confidential purpose.

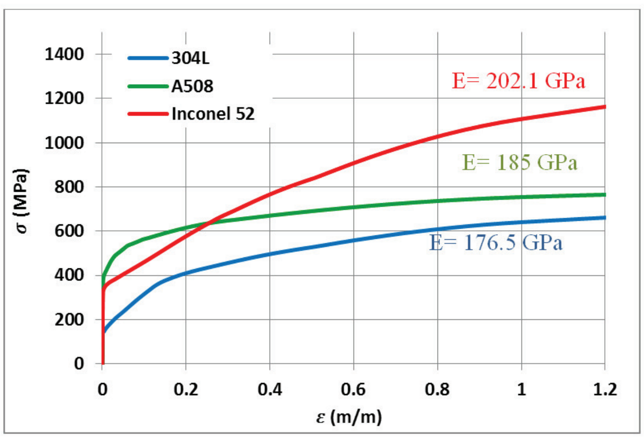

Figure 2. Tensile curves at 300°C

NUMERICAL VALIDITY OF THE J PARAMETER CALCULATION FOR A CRACK LOCATED ON A MULTI-MATERIAL INTERFACE

General methodology

Prior to the assessment of residual stress in DMW, it is important to briefly remind the numerical validity demonstration of the J calculation for a crack located on a multi-material interface is numerically valid [4].

A conventional crack was considered, parallel to the multi-material interface, located in the ferritic steel (A508) or in the nickel based alloy (Inconel 52), at a distance d_i from the interface. This distance varied from 1 to 0 mm, that is to say at the interface.

To calculate *J* parameter, three different kinds of integration paths were considered, in G-Theta method, for each case where the crack was not located at the interface (Figures 3 & 4) – *n* denotes here the number of elements along the ligament in the integration path, which is also the number of elements between the crack lips and the DMW interface:

- One path only contains one material ($n < 10$);
- One path only contains one material but is in contact with the interface ($n = 10$);
- One path crosses the interface ($n > 10$).

Also, different mesh sizes around the crack tip and integration path sizes were considered.

First, we attributed the A508 steel properties to all materials. Indeed, an elastic analytical solution exists to calculate the *J* parameter for an axial loading. This first step was very important since it was used to validate the mesh and the calculation. Also, the calculation of *J* is well known in homogeneous materials and the value is supposed to be stable through the fictional interface since we were considering only one material. Thus, all cases with the different loadings were first treated as homogenous material (A508).
Afterwards, the respective elastic properties of each material were attributed to each part and the *J* parameter calculated again for each type of loading (axial stress, internal pressure, thermal shock or combined). This step allowed us to conclude about the impact of a heterogeneous path on the G-theta method to calculate the elastic *J* parameter. Indeed, for the case where the crack was located at the interface, the integration path was obviously composed of different materials: the objective was to make sure the *J* parameter was still independent of the integration path despite the different materials.
For each case, the *J* parameter was calculated in order to evaluate the convergence at the interface and check if its evolution was continuous through the interface.

Thus, considering the elastic approach, we can sum up this methodology with four major steps:

1- Check the validity of the mesh and calculation;
2- Check the *J* independence to the integration path;
3- Calculate the *J* values close to the interface and at the interface;
4- If the evolution of the *J* parameter is continuous through the interface, then we can conclude that the calculation at the interface can be considered as numerically valid.

Finally, steps 1 to 4 were performed again considering elastic-plastic materials in order to validate the numerical validity of the *J* parameter.

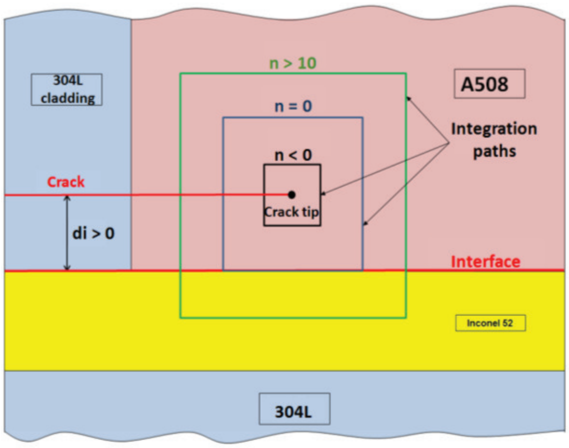

Figure 3. Different integration paths

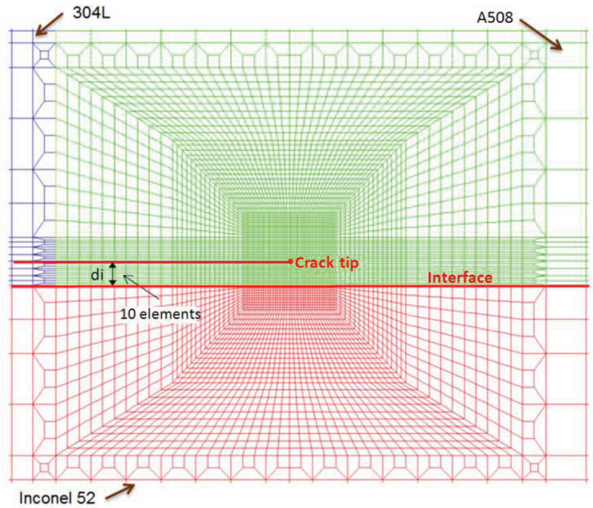

Figure 4. Example of mesh around the crack tip for di=0.25 mm (element size = 25 µm)

It is important to notice that all calculations were performed with each F.E. code, CASTEM® and SYSTUS®. As a matter of fact, this choice was made for an industrial purpose and allowed making sure results were the same and correct. 2D axisymmetric models were used for all cases.
Table 4 gives all the simulated cases for that topic. All of them were treated with the methodology previously described. Only a couple of them were presented in [4] (in black letters) but the conclusion was the same for all of them.

Table 4: Considered cases

Loading	Materials behavior	Model	Mechanical properties
Axial stress	Elastic	Homogeneous material	At 300 °C
		Multi-material	
	Elastic-plastic	Homogeneous material	
		Multi-material	
Internal pressure	Elastic	Homogeneous material	At 300°C
		Multi-material	
	Elastic-plastic	Homogeneous material	
		Multi-material	
Axial stress + Internal pressure	Elastic	Homogeneous material	At 300°C
		Multi-material	
	Elastic-plastic	Homogeneous material	
		Multi-material	
Thermal shock	Elastic	Homogeneous material	Depending on the temperature
		Multi-material	
	Elastic-plastic	Homogeneous material	
		Multi-material	
Thermal shock + axial stress +internal pressure	Elastic	Homogeneous material	Depending on the temperature
		Multi-material	
	Elastic-plastic	Homogeneous material	
		Multi-material	

Main results

The main obtained results are summed up here after:

- For elastic and elastic-plastic J calculation with G-Theta method, it is possible to use a heterogeneous integration path if the crack is parallel or directly at the multi-material interface.
- For elastic-plastic calculations, the used mesh size can have a significant impact on the J value, that is to say the J value can slightly fluctuate with mesh size change.
- The integration path independence, which is a major request of the G-Theta method, remains valid for elastic-plastic in confined plasticity.

- When there is loss of constraint due to important plasticity development, it is necessary to use a large enough integration path to calculate a valid *J* value and stay path independent.
- A good compromise for precision and calculation time would be for a ratio *mesh size* / R_0 between 0.0125 and 0.1 (with R_0 > 1.6 mm). Indeed, the difference with the converged *J* value would be inferior to 0.5%.
- Using SYSTUS® 2012 and CASTEM® 2012, the calculation of *J* value with G-Theta method, for a crack located on a multi-material interface, is numerically valid. Moreover, the results obtained for a same application are identical.

RESIDUAL STRESS FIELD

General analysis

After validating the calculation of the *J* parameter for a crack located on a multimaterial interface, it was proposed to enrich the considered model with a representative residual stress field. As a matter of fact, even if such a structure is heat treated after welding, residual stresses cannot be removed, essentially because of the physical properties between the different materials (E and α). The goal of our analysis is then to take those potential stresses into account in the analyses to evaluate their impact, which is not a trivial task. The conventional defect is only postulated at the interface between Inconel 52 and ferritic steel A508 since the toughness is the lowest in that area for ductile analyses [3].

In a R&D context, a very important work has been done at AREVA to simulate the welding of DMW and predict the residual stresses due to the manufacturing process [5]. Moreover, mock-ups have been realized and the residual stresses directly measured with different method (deep hole drilling, neutron diffraction). Regarding the fracture mechanics problematic, we are focusing on axial stresses which are perpendicular to the interface (and thus the assumed crack). In addition, for a strong material discontinuity such as a bi-metallic interface, experimental measurements can only give the stresses values accurately in the middle of the weld joint whereas we are considering a defect located at the interface between Inconel 52 and ferritic steel 508. As a consequence, only the results from the welding simulation can provide an estimation of the residual stresses for this area.

Thus, the mutual validation between the residual stresses values from the simulations and those from measurements can only be performed in the middle of the weld joint and in the base metals. Once this is achieved, the predicted values at the interface from modelling can then be used for our mechanical calculations. For that purpose, figure 5 shows the good agreement between the predicted (pink, dark blue and green lines for different modelling assumptions) and the measured (red circles) residual stresses values at the middle of the weld joint: the values calculated from the simulations are then considered as valid. Besides that, it can be noticed that, close to the interface, the stress increases at the inner surface side is due to the cladding.

It has been decided to define a reference residual stress field based on the predicted residual stresses values with two major constraints:

- It has to be simple enough to be easily introduced into FE models;
- For safety purpose, it also has to be a conservative envelop with the objective to obtain a representative level of stress corresponding to the elastic stress in mode I to open the crack.

If the residual stress field is imposed through an initial imposed strain field, for a complex case such as a DMW, this means that it is necessary to optimise the residual stress field. Another consequence is that it is not possible to define an envelope residual stress field for the whole thickness of such a structure:

- The residual stress field necessary becomes not auto-balanced, which is problematic for the axial stresses and thus the analysis of a circumferential defect;
- The length of application of the residual stress field through the thickness is not that important since the main point is to introduce the right level of stress at the Inconel 52 / A508 interface where the defect is located.

Therefore, a choice has been made and consists in defining two different residual stress fields for both internal and external defects. This solution favours the definition of simple and envelope stress distributions to introduce in the FE model. One of the main points is to describe correctly the stress level for a height fully covering the defect, that is to say a quarter of the thickness in our case (crack depth a = ¼ of the thickness). The rest of the residual stress field does not really matter as long as it is auto-balanced. For example, Figure 5 shows proposed conservative fits for internal and external defects regarding the modelling predicted level of axial residual stress.

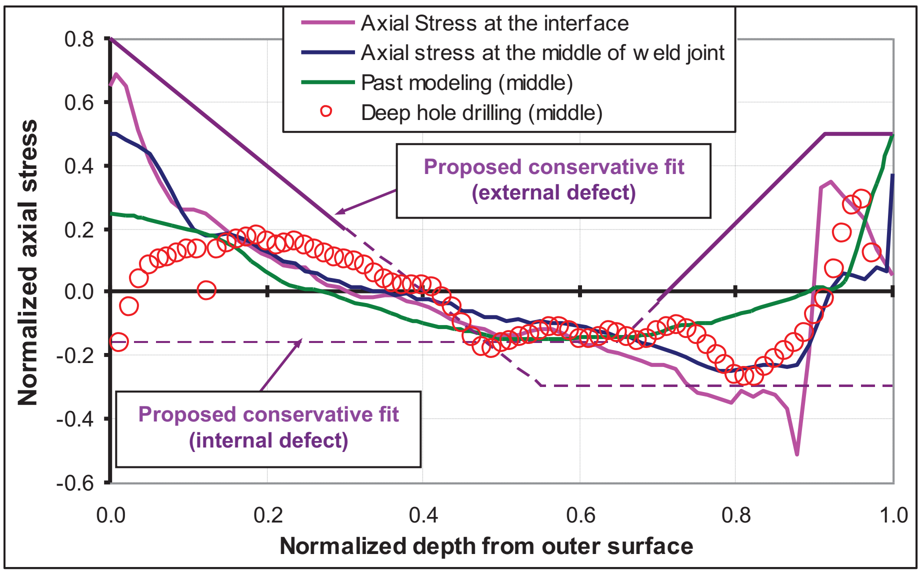

Figure 5. Residual stress fields at the Inconel 52 / A508 interface

Definition of three different reference residual stress fields

In that paper, for parametric study, three different axial residual stress fields have been defined and considered for FE modelling with internal surface defect (Figure 6a).

- RS field #1 represents a linear stress gradient with a maximum value enveloping the maximum calculated value (Max[RS field #1] = $0.8 \cdot \sigma_y^{(I52)}$).
- RS field #2 represents a three parts linear stress gradient with the same maximum value (Max[RS field #2] = $0.8 \cdot \sigma_y^{(I52)}$).
- RS field #3 represents the envelope residual stress field defined from the predicted values (Figure 5). The maximum stress value corresponds to Max[RS field #3] = $0.5 \cdot \sigma_y^{(I52)}$ at the inner surface.

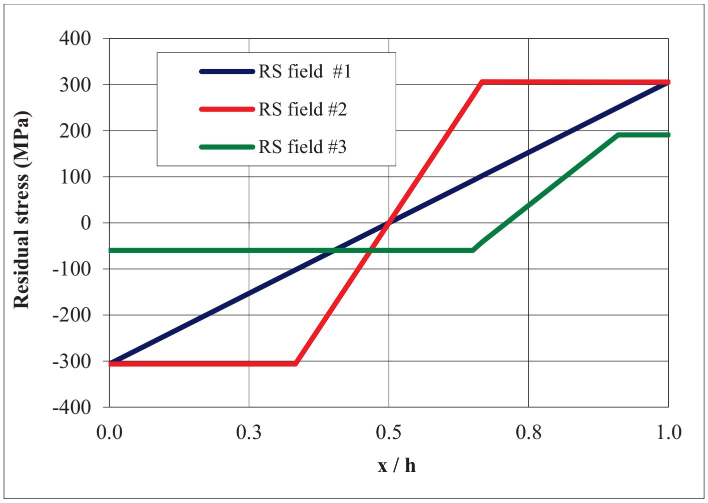

Figure 6. Three different considered axial residual stress fields

INTRODUCTION OF THE RESIDUAL STRESS FIELD INTO THE FE MODEL

To take a residual stress field into account with the considered FE model, the best practice is to introduce it through initial strains only [6]. It could be possible to use an equivalent thermal field but, the analysis of the structure with combined loads (mechanical and thermal shock loading) would become very difficult to perform. Therefore, a possibility is to use an equivalent thermal field to calculate the initial strains and to introduce directly those initial strains at the beginning of the FE analysis. Such an approach also allows the consideration of the strains corresponding only to the axial direction (uniaxial condition) or of the strains for both axial and circumferential directions (bi-axial condition). Our complete methodology adopted to perform a FE analysis with residual stress is the following:

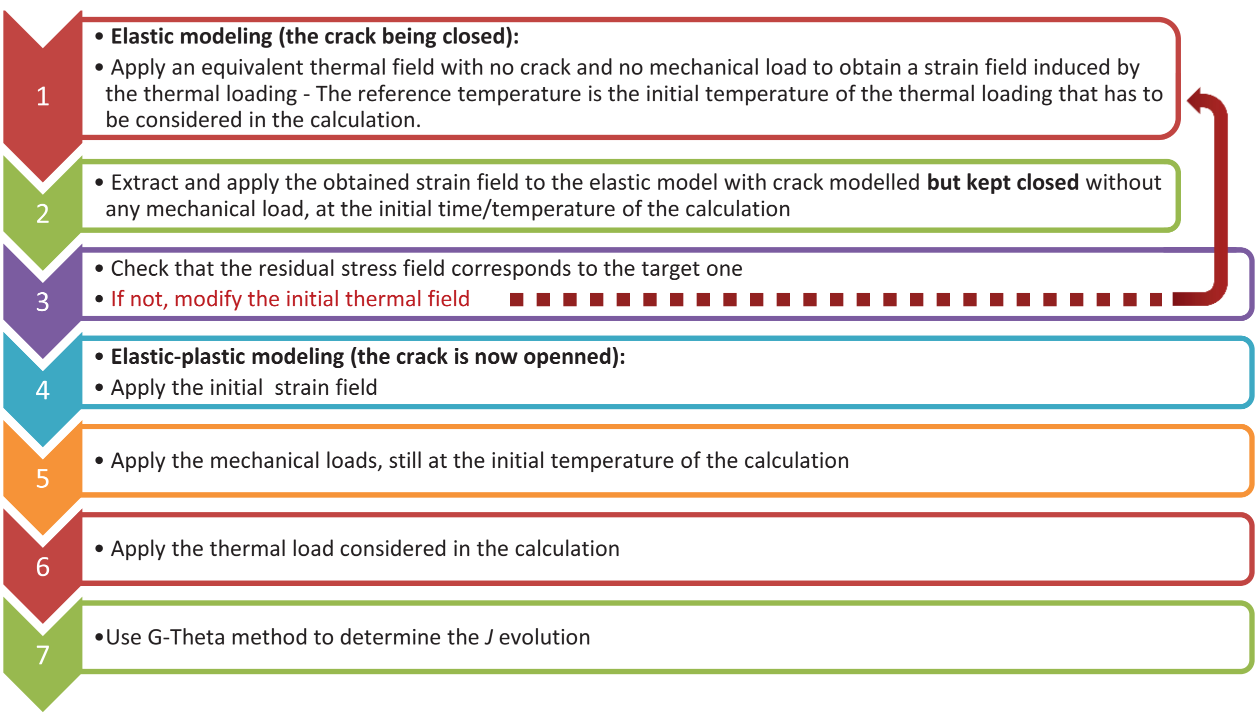

As an example, for the step 3 of the methodology, Figure 7 shows the obtained residual stress RS field #3 compared to the target one. A good agreement can be noticed and RS field #3 is correctly modelled.

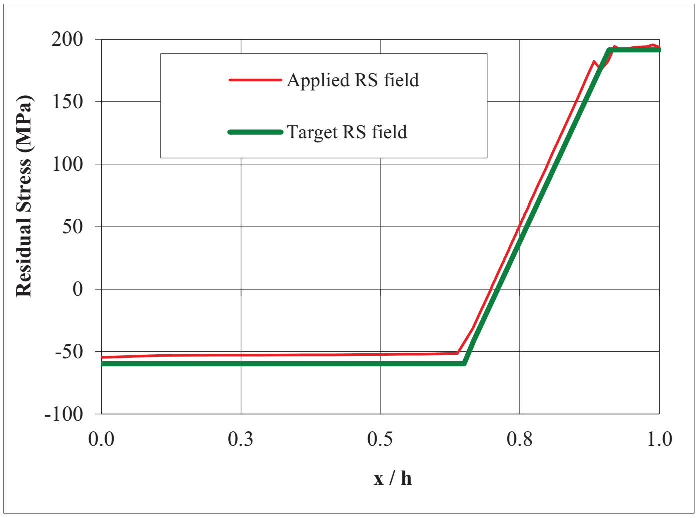

Figure 7. Comparison of the target and obtained residual stress fields for RS field #3

In the following calculations, the different residual stress fields have the following properties:

- RS field #1 is obtained from an equivalent thermal field and is thus bi-axial;
- RS field #2 is used with two configurations, that is to say bi-axial or uniaxial;
- RS field #3 is uniaxial.

FE ANALYSES - CALCULATION OF J WITH RESIDUAL STRESS

Boundary conditions and loadings

The model is still 2D axisymmetric and all the materials are taken into account. For each case, the structure is thus multi-material. Their properties are taken at 300°C (Figure 2). The crack is located at the Inconel 52/A508 interface at the internal surface (a=20 mm).

As mechanical load, an axial stress is considered and is applied as a pressure of 100 MPa (Figure 8). In addition, a cold thermal shock is applied on the internal skin of the structure. As for the external surface of the structure, it is submitted to adiabatic condition.

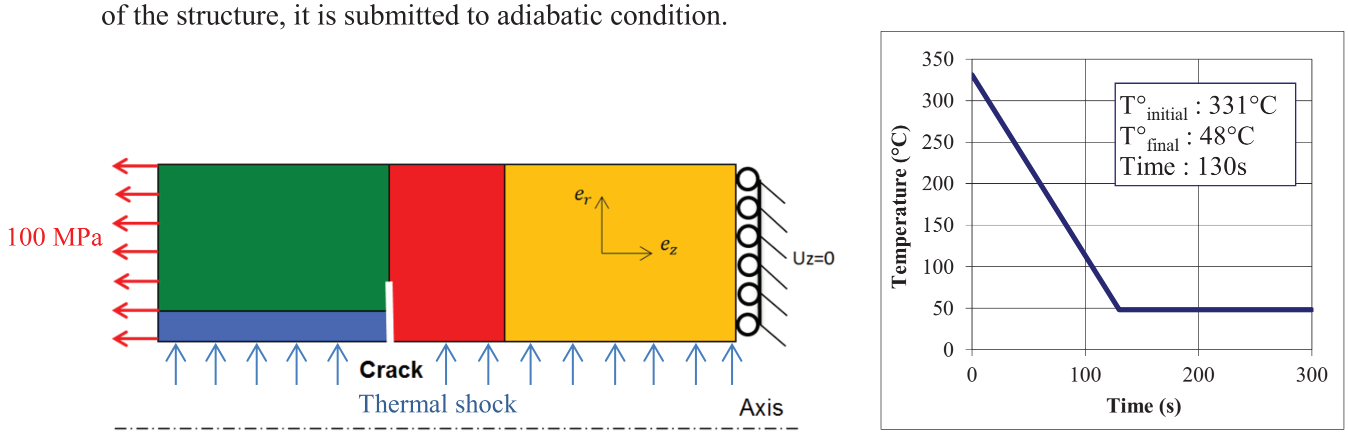

Figure 8. Boundary conditions and loadings

For each case, the FE analyses treat one configuration without any residual stress field and then all the presented residual stress fields.

Results

Figure 9a shows the calculated evolutions of J for the different configurations for a pure elastic behaviour. For those elastic calculations, it can be seen that the amplification of J is directly linked to the level of residual stress. Indeed, according to Figure 6, the most severe residual stress field is RS field #2, then RS field #1 and finally RS field #3. The same order can be noticed from Figure 9a. Moreover, there is no significant difference when considering uniaxial or biaxial residual stress field: both evolutions for RS field #2 are exactly the same. For RS field #2, the maximum J value is three times higher than without any residual stress.

Figure 9b shows the same results for elastic-plastic calculations. The evolutions of J are still in the same order, that is to say that the most severe residual stress field leads to the highest J value. However, in that case, a difference can be noticed when a residual stress field is considered as uniaxial or biaxial. Indeed, the two evolutions for RS field #2 are different and the J values are slightly higher for the biaxial one. Besides, it can be noticed that the J values decrease a lot compared to the elastic ones: the maximum ratio between the cases without residual stress and RS field #2 is reduced to 2. From an industrial point of view, the most interesting result is for RS field #3, which corresponds to the conservative stress field determined from the simulations: it can be seen that this severe envelope leads to an increase of the maximum value of J compared to the case without any residual stress. However, the difference does not exceed 20%.

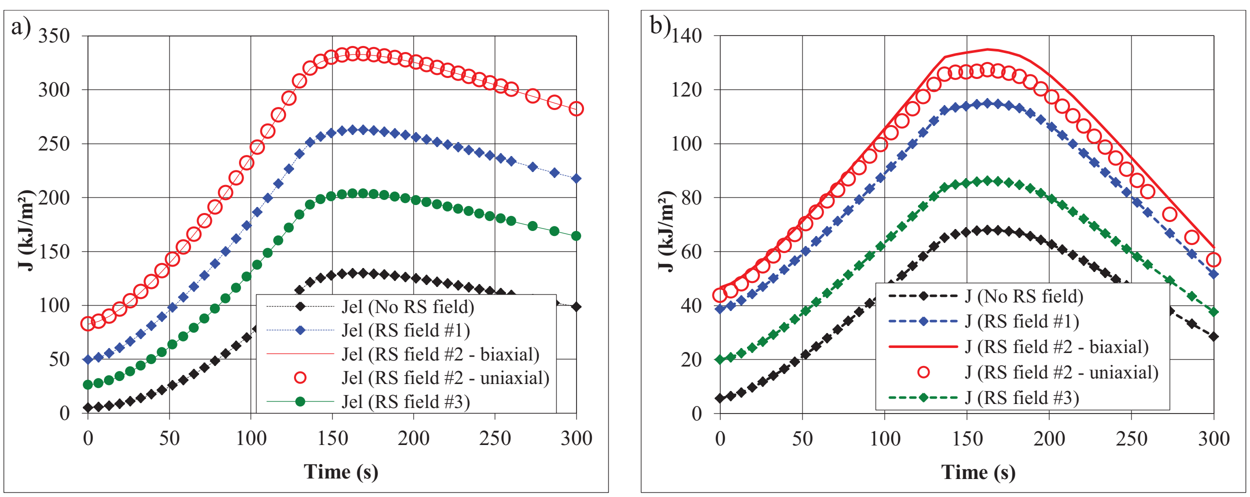

Figure 9. J evolution for the different cases a) Elastic b) Elastic-plastic

Regarding the k_{th} coefficient, the parameter representative of through thickness loading relaxation [7], it is shown that residual stresses are significantly relaxed with plasticity and the presence of the imposed mechanical loading (time step corresponding to t = 0 s on fig. 10):

$$k_{th} = \frac{\sqrt{J^{RS+m+th}} - \sqrt{J^m}}{\sqrt{{J_{el}}^{RS}} + \sqrt{{J_{el}}^{th}}}$$

Further, figure 10 shows that when the residual stresses are more important, the k_{th} parameter decreases at the initial time and also during the whole considered transient. Moreover, uniaxial residual stress slightly reduces the k_{th} parameter compared to the biaxial one.

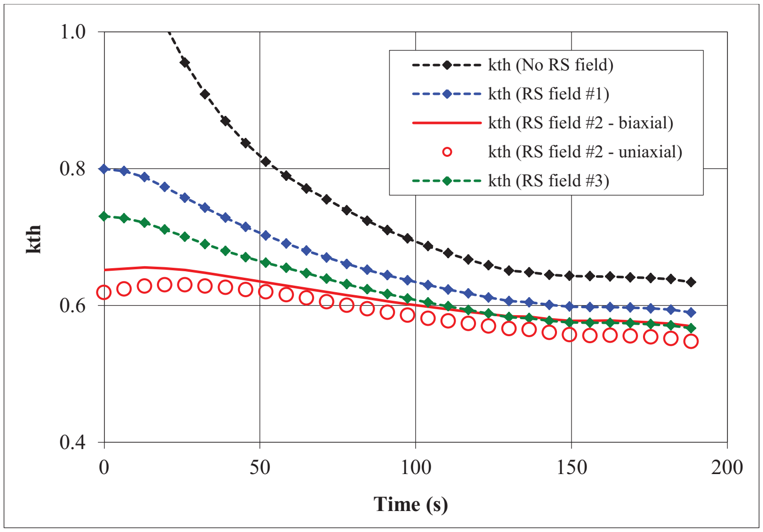

Figure 10. k_{th} evolutions for the different cases

Validation of the J calculation with residual stresses

For validation purpose, the presented FE calculations have been performed with three different integration path sizes to make sure the *J* values are reliable and converged. Figure 11 shows the evolutions of J from those different calculations for the case without any residual stress field which has been validated in [4] and the case with RS field #1.

As it can be noticed, from the initial time to the maximum *J* value during the thermal shock, the curves for the configuration with RS field #1 are very similar to those without any residual stress except they are translated due to the increase of stress at the initial time. Moreover, for the maximum J values, the three calculations of both configurations give the same value and the difference is negligible (< 0.1 %). As a consequence, the calculation of *J* for such a complex configuration (crack located at a multi-material interface, elastic-plastic behaviours, combined loads, residual stress field etc…) is considered as numerically valid.

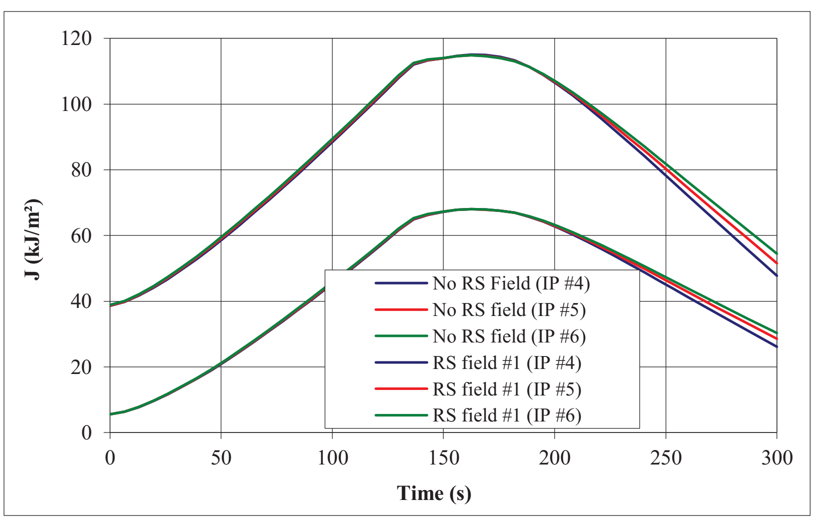

Figure 11. Comparison of J evolution for different integration path sizes and with/without residual stresses

CONCLUSION

The objective of this paper was to complete the work presented in a previous paper [4] about the validation of the *J* parameter in a very complex configuration: a conventional defect located at the interface of a dissimilar metal weld representative of the weld between the EPR™ pressure vessel (A508 ferritic steel) and the coolant piping system (304L austenitic steel). Indeed, the main objective was to investigate the residual stresses aspect. The first goal was to determine a realistic and simple fit for that type of DMW, but still conservative for safety purpose. A first fit has been proposed, based on validated welding simulations results. Then, a methodology to introduce residual stresses into FE models has been proposed. Different residual stress fields have been defined and a parametric study has been performed through FE analyses to evaluate the different configurations. The elastic calculations have shown that a higher residual stress field leads to a higher value of *J*. The same observation has been done with elastic-plastic calculations. However, it has been demonstrated that the proposed realistic residual stress fit does not impact the maximum value of *J* more than 20% with elastic-plastic behaviour. Moreover, it has been shown that considering the residual stresses in elastic-plastic calculations does not impact the maximum *J* value as much as with elastic ones. Also, using a biaxial stress field is more conservative than a uniaxial one. Besides, a few investigations have been done about the impact of residual stresses on k_{th} parameter and have shown that it decreases a lot when they are taken into account. Another major conclusion of this work is that the *J* calculation is numerically valid for such an application. Finally, this paper only presents the beginning of the next studies about residual stress fields. As a matter of, more work will be done to determine stress fields for different types and geometries of DMW, propose conservatives fits and check the influence of all parameters in the FE modelling. Also, residual stresses will be introduced in 3D FE models.

REFERENCES

[1] A. Blouin et al. (2014), “Brittle fracture analysis of a dissimilar metal weld”, *Engineering Fracture Mechanics 131* pp 58–73.

[2] P. Joly, M. Yescas and E. Keim (2014), “Fracture toughness in the ductile-brittle transition and thermal behaviour of decarburized heat affected zone of alloy 52 Dissimilar Metal Welds of nuclear components”, PVP2014-29044, *ASME Pressure Vessel and Piping Division conference,* Anaheim, California, USA.

[3] M. Bourgeois et al. (2014), “Four point bending test on an EPR type DMW pipe containing a through-wall defect: experimental and numerical analysis from small specimens until pipe scale”, PVP2014-28321, *ASME Pressure Vessel and Piping Division conference,* Anaheim, California, USA.

[4] A. Blouin, S. Chapuliot and W. Hamouche (2014). “Evaluation of the numerical validity of the J parameter for a crack located on a multi-material interface”, *ASME Pressure Vessel and Piping Division conference*, Anaheim, California, USA.

[5] P. Gilles et al. (2013), “Methodology for numerical welding simulation validation: the Dissimilar metal weld case”, PVP2013-97475, *ASME Pressure Vessel and Piping Division conference*, Paris, France.

[6] Marie et al. (2013), “Benchmark on residual stress modeling in fracture mechanics assessment”, PVP2013-97177, *ASME Pressure Vessel and Piping Division conference*, Paris, France.

[7] S. Chapuliot et al. (2015), “RSE-M/RCC-MRx Analytical scheme for the J parameter calculation on cracked pipes and vessels submitted to through thickness thermal loading”, *SMIRT conference*, Manchester, UK.

[8] CAST3M, CEA,. www-cast3m.cea.fr

[9] SYSTUS 2012, ESI, www.esi-group.com/software-services/virtual-environment/cfd-multiphysics/systus